Available online at www.sciencedirect.com
ScienceDirect
Journal of Power Sources 158 (2006) 1358–1364
JOURNAL OF POWER SOURCES
www.elsevier.com/locate/jpowsour

Synthesis and characterization of spinel $Li_4Ti_5O_{12}$ anode material by oxalic acid-assisted sol–gel method

Yan-Jing Hao, Qiong-Yu Lai *, Ji-Zheng Lu, Hong-Li Wang, Yuan-Duan Chen, Xiao-Yang Ji

College of Chemistry, Sichuan University, Chengdu 610064, PR China

Received 4 July 2005; received in revised form 26 August 2005; accepted 13 September 2005
Available online 21 November 2005

Abstract

Anode material $Li_4Ti_5O_{12}$ for lithium-ion batteries has been prepared by a novel sol–gel method with oxalic acid as a chelating agent and Li_2CO_3 and tetrabutyl titanate $[Ti(OC_4H_9)_4]$ as starting materials. Various initial conditions were studied in order to find the optimal conditions for the synthesis of $Li_4Ti_5O_{12}$. Oxalic acid used in this method functioned as a fuel, decomposed the metal complexes at low temperature and yielded the free impurity $Li_4Ti_5O_{12}$ compounds. Thermal analyses (TG–DTA) and XRD data show that powders grown with a spinel structure (*Fd*3*m* space group) have been obtained at 800 °C for 16 h. SEM analyses indicated that the prepared $Li_4Ti_5O_{12}$ powders had a uniform cubic morphology with average particle size of 200 nm. The influence of synthesis conditions on the electrochemical properties was investigated and discussed. The discharge capacity of $Li_4Ti_5O_{12}$ synthesized with an oxalic acid to titanium ratio $R = 1.0$ was 171 mAh g^{-1} in the first cycle and 150 mAh g^{-1} after 35 cycles under an optimal synthesis condition at 800 °C for 20 h. The very flat discharge and charge curves indicated that the electrochemical reaction based on Ti^{4+}/Ti^{3+}redox couple was a typical two-phase reaction.
© 2005 Elsevier B.V. All rights reserved.

Keywords: Lithium-ion battery; Anode material; $Li_4Ti_5O_{12}$; Sol–gel method; Oxalic acid

1. Introduction

Intercalation electrode materials for lithium-ion batteries have been extensively investigated worldwide in the past 20 years. Spinel $Li_4Ti_5O_{12}$ [1–5] is a promising anode material for lithium-ion batteries. This material exhibits characteristic properties, including very flat discharge and charge curves and a small structural change during charge–discharge processes. The material has a theoretical specific capacity of 175 mAh g^{-1} and exhibited a practical specific capacity as high as 150–160 mAh g^{-1} after 100 deep discharge cycles [1–5]. During the process of Li^+ intercalation and de-intercalation, the cubic symmetry of the parent spinel is unaffected by lithiation; the lattice parameter (8.36 Å) and unit-cell volume are virtually unaltered by the phase transition [1]. The lack of significant change to the crystallographic parameter is remarkable and provides a structure that is extremely tolerant to electrochemical cycling. At the same time, the improved safety and reliability of the spinel compared with that of carbon electrodes make the lithium-ion batteries using $Li_4Ti_5O_{12}$ material as anode suitable to electric vehicle (EV) and power storage batteries.

$Li_4Ti_5O_{12}$ powders are usually synthesized by a solid-state reaction of lithium and titanium salts [1–12]. This method was generally preferred because the synthesis procedures are simple. But there are some disadvantages of solid-state methods such as larger particle size of the products, inhomogeneous distribution, lack of stoichiometry control, etc. These disadvantages can be overcome by sol–gel method [13–16], which offers products with a homogeneous distribution of uniform, sub-micron size particles with good stoichiometry control. Bach et al. [13] have synthesized spinel $Li_4Ti_5O_{12}$ via a sol–gel process in non-aqueous media and the electrochemical behavior of the sol–gel $Li_4Ti_5O_{12}$ spinel oxide is examined. Shen et al. [14] report the first synthesis of $Li_4Ti_5O_{12}$ nanocrystalline using acetate acid as a chelating agent by sol–gel method. Thin films of $Li_4Ti_5O_{12}$ was prepared from precursors obtained by a sol–gel process using poly(vinylpyrrolidone) (PVP) as a polymer binding with Li^+ ions and metal cations by Rho et al. [15]. The addition of PVP polymer is helpful to form a uniform sol solution. In our previous work, we report the synthesis of spinel $Li_4Ti_5O_{12}$

* Corresponding author. Tel.: +86 28 85416969; fax: +86 28 85416969.
E-mail address: laiqy5@hotmail.com (Q.-Y. Lai).

0378-7753/$ – see front matter © 2005 Elsevier B.V. All rights reserved.
doi:10.1016/j.jpowsour.2005.09.063

material by a sol–gel method using triethanolamine (TEA) as a chelating agent [16]. Sub-micron $Li_4Ti_5O_{12}$ powders with narrow particle size (100 nm) distribution and superior dispersion were achieved. Though a lot of work has been done in these sol–gel methods, further research in investigating the effect of the chelating agent on the particle size and morphology of product and its electrochemical properties was still needed.

Oxalic acid has been used in the solution chemistry method to prepare oxides such as TiO_2 [17], $LiMn_2O_4$ [18], $Li_xNi_{0.8}Co_{0.2}O_2$ [19] and others. But it has not been used in the preparation of spinel $Li_4Ti_5O_{12}$ to our best knowledge. In this paper, $Li_4Ti_5O_{12}$ was prepared by a novel sol–gel route using oxalic acid as a chelating agent and the effect of the chelating agent on the particle size of the products, and on its electrochemical properties, was investigated too. By using oxalic acid, we obtained fine $Li_4Ti_5O_{12}$ powders with excellent reliability and cyclability. And by adjusting the quantity of the oxalic acid in the solutions, we can control the morphology and particle size of the powders, thus controlling the electrochemical properties of the products.

2. Experimental

2.1. Preparation of $Li_4Ti_5O_{12}$

A typical sol–gel synthesis of $Li_4Ti_5O_{12}$ with oxalic acid as a chelating agent was performed the following way. Stoichiometric amounts of Li_2CO_3 and tetrabutyl titanate [$Ti(OC_4H_9)_4$] were dissolved in alcohol, respectively, to obtain solutions A and B. An ethanol solution of oxalic acid was added to a mixed solution of A and B under constant stirring to obtain a sol, such that the oxalic acid to titanium ratio, R, were varied at 0.25, 0.5, 0.75, 1.0, 1.25 and 1.5. The solution was then stirred for several hours to obtain a gel. The resulting gelatin was dried at 80 °C over 6 h to extract out excess ethanol and yield organic precursors. The gel precursors were preheated at 500 °C for 6 h in air and then calcined at different temperatures for different time, then cooled in the furnace to room temperature to obtain final powders.

The thermal decomposition behavior of the precursors was examined by means of thermogravimetry (TG) and differential thermal analysis (DTA) using a EXSTAR6000 analyzer (SEIKO) with simultaneous recording of weight losses (gravimetric thermal analysis) and temperature variations (differential scanning calorimetry). Powder X-ray diffraction (XRD) data were collected on a Rigaku D/MAX-rA diffractometer with Cu Kα radiation (λ = 1.5418 Å), operating at 40 kV and 100 mA. The scanning electron microscope (SEM, Hitachi_S-450, Japan) was used to observe the grain morphology and particle size. The electrochemical properties of $Li_4Ti_5O_{12}$ electrodes were determined from Li/1 M $LiPF_6$ in ethylene carbonate and diethyl carbonate (EC-DEC 1:1, w/w)/$Li_4Ti_5O_{12}$ cells by using a LAND Battery Program-Control Test System. The $Li_4Ti_5O_{12}$ electrodes were fabricated by mixing 85:10:5 (w/w) ratio of active material, a carbon (acetylene black) electronic conductor and polyvinylidene fluoride (PVDF) binder, respectively, using N-methyl-2-pyrrolidine (NMP) as the solvent. After drying the obtained slurry overnight under vacuum at 80 °C, the mixture was pressed onto a stainless steel grid. Lithium was used as the counter electrode. The cells were assembled in a glove box. All the electrochemical tests were carried out at room temperature. Charge–discharge cycle tests were performed at a constant current density of 0.5 mA cm^{-2} over a potential range between 1.0 and 2.5 V.

3. Results and discussion

3.1. Thermal analysis

In order to measure the exact phase formation and/or crystallization temperature of the $Li_4Ti_5O_{12}$ samples, TG-DTA measurements were carried out on the as-obtained xerogel. Fig. 1 shows the TG-DTA curves, which display the formation temperature of the oxide $Li_4Ti_5O_{12}$ grown by the oxalic acid-assisted solution method with oxalic acid to titanium molar ratio $R = 1.0$. The first step of weight loss, observed between room temperature and 120 °C, is mainly due to the vaporization of water and ethanol, and the liberation of butyl alcohol from the alkoxide. They correspond to an endothermic peak around 100 °C on the DTA curve. After this step, two exothermic transformations are observed from the DTA graph. The first exothermic process is centered at 422.7 °C, which is attributed to the combustion of the xerogel precursor and release of CO_2 and H_2O gases. The xerogel precursor was mainly composed of $TiOC_2O_4{\cdot}xH_2O$, $TiO_2{\cdot}2H_2O$, $Ti(OH)_3C_2O_4Li$, $Li_2C_2O_4{\cdot}2H_2O$ and Li_2CO_3 according to the following gelation process:

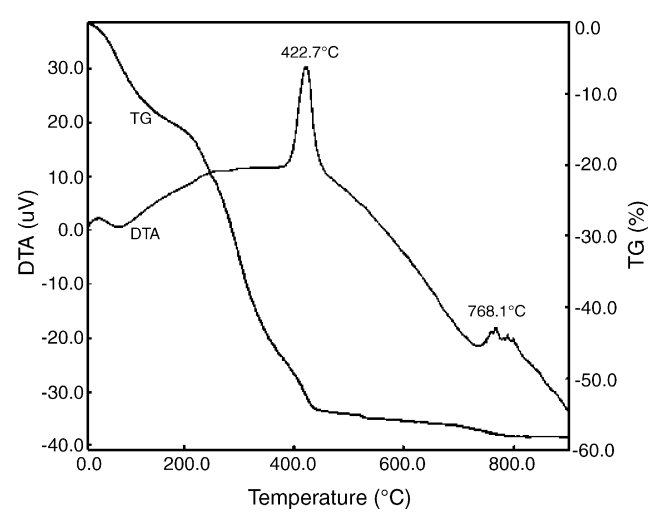

$$(C_4H_9O)_4Ti + 4H_2O \Leftrightarrow TiO_2{\cdot}2H_2O + 4C_4H_9OH \quad (1)$$

$$TiO_2{\cdot}2H_2O + H_2C_2O_4 \Leftrightarrow TiOC_2O_4{\cdot}xH_2O + (3-x)H_2O \quad (2)$$

$$Li_2CO_3 + H_2C_2O_4 + H_2O = Li_2C_2O_4{\cdot}2H_2O + CO_2 \quad (3)$$

Fig. 1. TG-DTA curves of the $Li_4Ti_5O_{12}$ precursor prepared by oxalic acid with $R = 1.0$.

$$Li_2CO_3 + 2(C_4H_9O)_4Ti + 2H_2C_2O_4 + (5 + 2x)H_2O = 2Ti(OH)_3C_2O_4Li \cdot xH_2O + 8C_4H_9OH + CO_2 \quad (4)$$

The decomposition process mainly occurred at this temperature range (250–500 °C) with a weight loss of 40.85%. The decomposition reactions in this range may be proceeding as given below:

$$TiOC_2O_4 \cdot xH_2O + 1/2O_2 = TiO_2 + 2CO_2 + xH_2O \quad (5)$$

$$Li_2C_2O_4 \cdot 2H_2O + 1/2O_2 = Li_2CO_3 + CO_2 + 2H_2O \quad (6)$$

$$2Ti(OH)_3C_2O_4Li \cdot xH_2O + O_2 = 2TiO_2 + Li_2CO_3 + 3CO_2 + (3 + 2x)H_2O \quad (7)$$

This indicates that the initiation of the crystallization reaction at about 500 °C and the combustion of oxalic acid supplies adequate heat energy for initiating the crystallization of $Li_4Ti_5O_{12}$. The final weight loss from 700 to 800 °C is mainly attributed to the thermal decomposition of residue carbonate phases and the completion of the crystallization reaction. It corresponds to the following reaction:

$$2Li_2CO_3 + 5TiO_2 = Li_4Ti_5O_{12} + 2CO_2 \quad (8)$$

There is no weight loss after 800 °C, up to a temperature of 900 °C.

3.2. XRD analysis

The XRD patterns of the samples obtained at different temperatures for 20 h are presented in Fig. 2. The molar ratio of oxalic acid to titanium R is 1.0. It can be seen from Fig. 2(a) that the sample obtained at 500 °C is a mixture phase of $Li_4Ti_5O_{12}$ and anatase TiO_2 (main phase). When the heating temperature was 600 °C, the diffraction peaks of $Li_4Ti_5O_{12}$ phase and TiO_2 phase gradually enhanced simultaneously [Fig. 2(b)]. When the precursor was calcined at 700 °C for 20 h [Fig. 2(c)], the diffraction peaks of $Li_4Ti_5O_{12}$ gradually sharpened with the increase of temperature. There is, however, an extra diffraction peak at $2\theta = 27.4°$, indicating that the presence of a small amount of unreacted TiO_2. The XRD pattern of the samples obtained at 800 °C exhibit the characteristic diffraction lines of $Li_4Ti_5O_{12}$ without any miscellaneous phase, which completely match that of the spinel structure listed in JCPDS file no. 26–1198, confirming that a pure compound of $Li_4Ti_5O_{12}$ formed. This result was consistent with the TG-DTA results. The cubic lattice parameter of $Li_4Ti_5O_{12}$ was calculated to be $a = 8.364$ Å, which is in good agreement with those obtained by Ohzuku et al. [1] and Wang et al. [3].

Fig. 3 shows the X-ray diffraction patterns of spinel $Li_4Ti_5O_{12}$ calcined at 800 °C for different times with oxalic acid to titanium molar ratio $R = 1.0$. The results indicated that the TiO_2 phase appeared in the sample obtained at 800 °C for l2 h. The pure $Li_4Ti_5O_{12}$ phase can be obtained at 800 °C for 16 h or more.

In order to investigate the effect of the quantity of chelating agent on the purity of $Li_4Ti_5O_{12}$ spinel, the precursor materials were prepared with different molar ratios of oxalic acid to titanium. Fig. 4 shows XRD patterns for the $Li_4Ti_5O_{12}$ synthesized

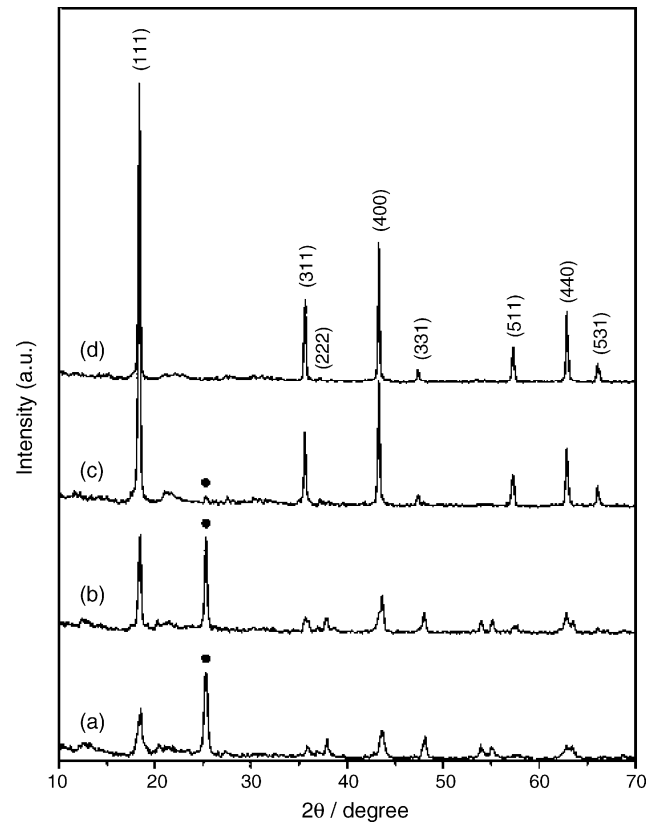

Fig. 2. X-ray diffraction patterns of $Li_4Ti_5O_{12}$ prepared at different temperatures for20 h with $R = 1.0$: (a) 500 °C, (b) 600 °C, (c) 700 °C and (d) 800 °C. (●) Anatase TiO_2.

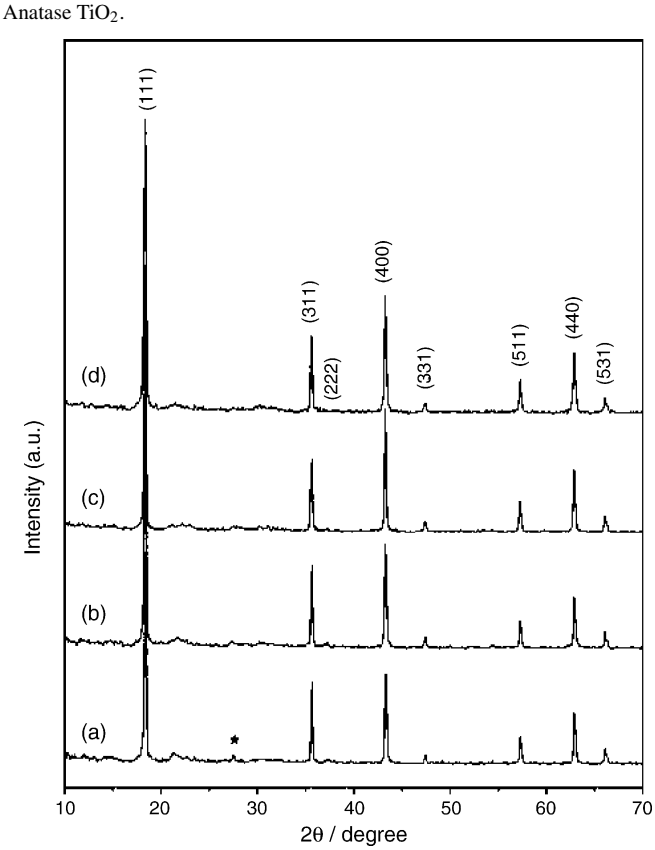

Fig. 3. X-ray diffraction patterns of $Li_4Ti_5O_{12}$ prepared at 800 °C for different time with $R = 1.0$: (a) 12 h, (b) 16 h, (c) 20 h, (d) 24 h. (*) Rutile TiO_2.

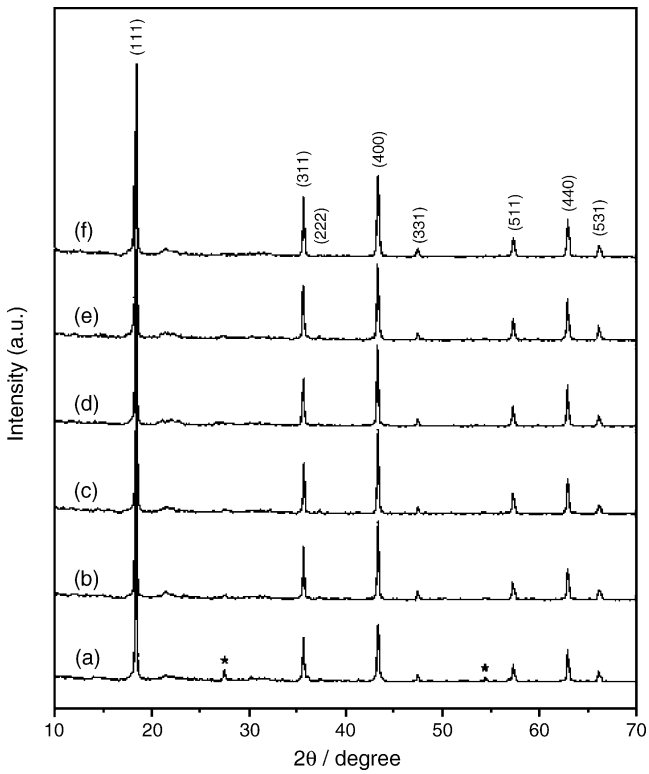

Fig. 4. X-ray diffraction patterns of $Li_4Ti_5O_{12}$ prepared at 800 °C for 20 h by different molar ratio *R*: (a) 0.25, (b) 0.5, (c) 0.75, (d) 1.0, (e) 1.25 and (f) 1.5. (*) Rutile TiO_2.

with oxalic to titanium ratio $R = 0.5$, 0.75, 1.0, 1.25 and 1.5 by calcination at 800 °C for 20 h in air after preheating. It can be seen from Fig. 4(a) that in the sample prepared with $R = 0.25$ exists a little amount of unreacted rutile TiO_2. All the other patterns exhibit no other than peaks for the $Li_4Ti_5O_{12}$ phase with *Fd*3*m* space group. The results indicated that the oxalic acid used acts as a chelating agent and also provides the local heat for the formation of the compound during the decomposition. The heat produced in the gel-combustion process makes the nucleation process complete at the early stage of the synthesis process. So the quantity of the chelating agent is very important for the synthesis of pure $Li_4Ti_5O_{12}$ powders. If the oxalic acid quantity is too small, the combustion heat becomes insufficient for the synthesis of the oxides. Higher temperature or longer time may be needed to form pure $Li_4Ti_5O_{12}$ powders at this condition.

3.3. SEM analysis

Fig. 5 presents the scanning electron micrographs (SEM) of $Li_4Ti_5O_{12}$ powders calcined at 800 °C for 20 h for different *R*-values. It can be seen in Fig. 5 that all the micrographs show homogeneous distribution of the particles without serious agglomeration. And the observed average particle size of the prepared $Li_4Ti_5O_{12}$ powders was different as the value of *R* increases from 0.5 to 1.0. In the case of the gel precursor with $R = 0.5$ [Fig. 5(a)], the average particle size of $Li_4Ti_5O_{12}$ powders was about 500 nm. When the oxalic acid to titanium ratio was increased from 0.5 to 1.0 [Fig. 5(b)], the average particle size decreased to about 200 nm. A further increase in *R* to 1.5 [Fig. 5(c)] caused the average particle size of prepared powders increased to about 300 nm. This indicated that the quantity of the chelating agent is important for the synthesis of $Li_4Ti_5O_{12}$ powders. It has great effect on the particle size of the obtained product, thus affecting the electrochemical properties of the $Li_4Ti_5O_{12}$ materials.

Patil et al. [17], who synthesized TiO_2 with oxalic acid as a chelating agent and a fuel, found that oxalic acid played an important role in the formation of micro-porous titania. According to Patil et al. [17], oxalic acid forms a mixed precursor, which acts as a substrate for the homogeneous distribution of the metal oxide phase. Upon calcination in air, the carbonaceous substrate is oxidized to carbon dioxide, leaving behind a finely divided oxide phase.

In our case, the oxalic acid had the similar effect. Oxalic acid was added as a complexing agent in the above methanolic solution. Oxalic acid could complex with TiO^{2+} to form a relatively stable complex for preventing the excessively rapid hydrolysis of TiO^{2+}. And then Ti-complex gradually hydrolyzed and polymerized to obtain a mixed precursor gel net-work which was composed of $[TiOC_2O_4{\cdot}xH_2O]$, $Ti(OH)_3C_2O_4Li{\cdot}xH_2O$ and $TiO_2{\cdot}2H_2O$. The gelation process has been described as reactions (1), (2) [20] and (4).

In the gel network, the final composition may be either a mixture of $TiOC_2O_4{\cdot}xH_2O$ and $Ti(OH)_3C_2O_4Li{\cdot}xH_2O$ or a mixture of $TiOC_2O_4{\cdot}xH_2O$, $Ti(OH)_3C_2O_4Li{\cdot}xH_2O$ and $TiO_2{\cdot}2H_2O$ depending on whether reaction (2) goes to completion or not, under the synthesis conditions. So we can control the amount of the $[TiOC_2O_4{\cdot}xH_2O]$, $Ti(OH)_3C_2O_4Li{\cdot}xH_2O$ and $TiO_2{\cdot}2H_2O$ in the final gel mixture by adjusting the amount of the chelating agent oxalic acid accoiding to reaction (2), thus controlling the particle size of the products. In our work, we choose to change the oxalic acid to titanium molar ratio *R* from 0.25 to 1.5.

Furthermore, the oxalic acid chelating agent acts as an organic fuel during the formation process of transition-metal oxide powders, decomposed the metal complexes at low temperature. The heat produced in the gel-combustion process makes the nucleation process complete at the early stage, leading to a narrow size distribution of the $Li_4Ti_5O_{12}$ powders. Upon calcination in air, the carbonaceous substrate is oxidized to evolve large amounts of gasses and the accompanying gas evolution helps break down large agglomerated particles and inhibit the continuous growth of the crystallite, leaving behind a finely divided oxide phase.

3.4. Electrochemical analysis

Fig. 6 shows the first charge–discharge curves between 1.0 and 2.5 V of $Li_4Ti_5O_{12}$ calcined at 800 °C for 20 h with the molar ratio of oxalic acid to titanium $R = 1.0$. As seen in Fig. 6, the profile exhibited extremely flat operating voltage at about 1.5 V (versus Li), which is consistent with the results of previous study [3]. The capacity of the flat voltage was 85.8% of the overall discharge capacity. During the subsequent charge process, a very flat charge curve at about 1.6 V (versus Li) can be observed

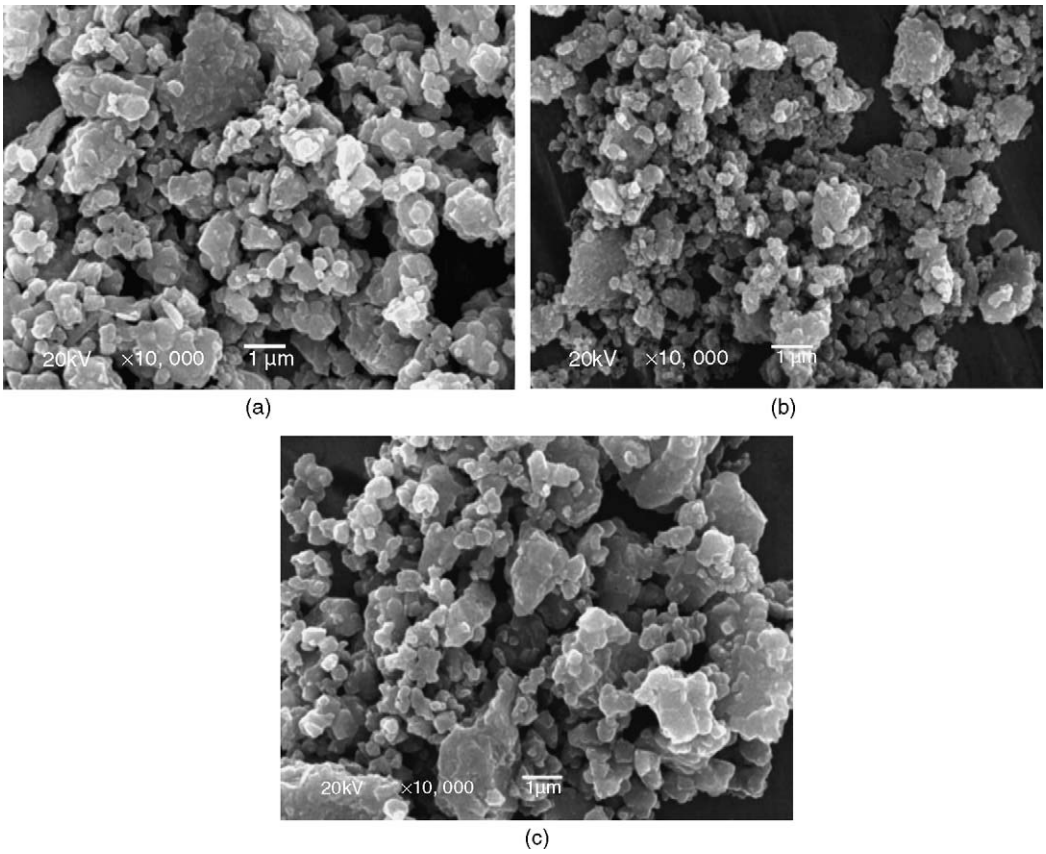

Fig. 5. SEM patterns of $Li_4Ti_5O_{12}$ prepared at 800 °C for 20 h by different molar ratio R of oxalic acid to titanium: (a) 0.5, (b) 1.0 and (c) 1.5.

and the discharge and charge voltage are close. This suggests a two-phase reaction based on the Ti^{4+}/Ti^{3+} redox couple. The electrochemical reaction can be described as [1]:

$$[Li]_{8a}[Li_{1/3}Ti_{5/3}]_{16d}[O_4]_{32e} + Li^+ + e^- \Leftrightarrow [Li_2]_{16c}[Li_{1/3}Ti_{5/3}]_{16d}[O_4]_{32e}$$

During the intercalation of Li-ions into the $Li_4Ti_5O_{12}$ structure, Li-ions begin to occupy 16c sites. Then Li-ions in the tetrahedral 8a sites also migrate to 16c sites. Eventually, all 16c sites are occupied by Li-ions.

Cycling performance of the compounds calcined at 600, 700 and 800 °C for 20 h with $R = 1.0$ are shown in Fig. 7. As evidenced by the X-ray diffraction studies, the compound calcined at 600 °C [Fig. 7(A)] showed poor electrochemical characteristics. In the first cycle, the discharge capacity was 135 mAh g^{-1}, and after 10 cycles, the discharge capacity decreased rapidly to 37 mAh g^{-1}. The main reason for the lower capacity was

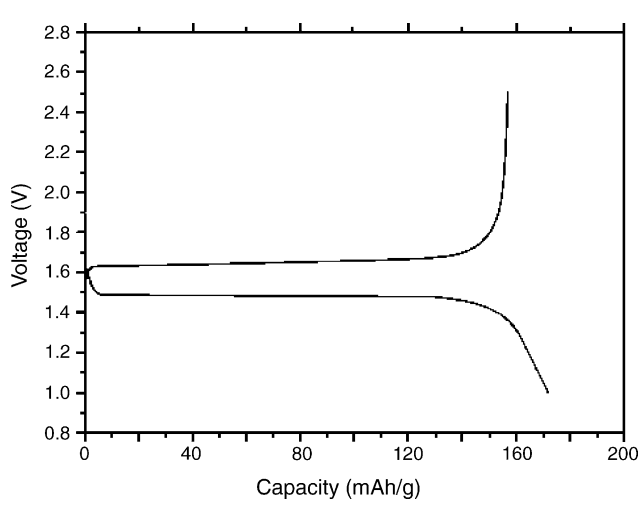

Fig. 6. The first charge–discharge curves of $Li_4Ti_5O_{12}$ prepared at 800 °C for 20 h with $R = 1.0$.

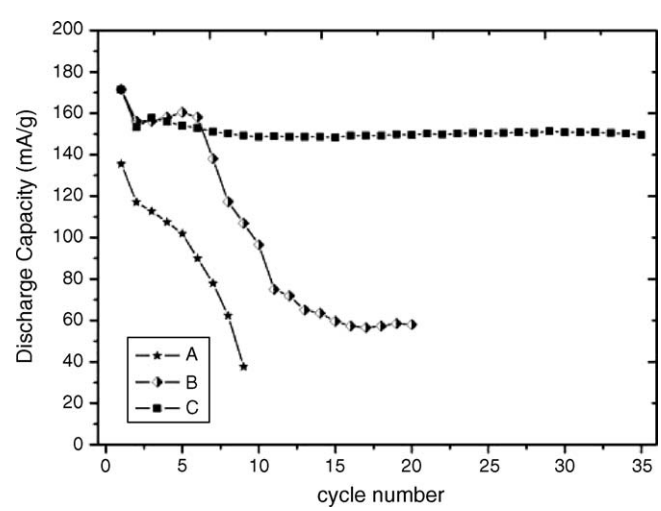

Fig. 7. Cycling performance of $Li_4Ti_5O_{12}$ prepared at different temperatures for 20 h with $R = 1.0$: (A) 600 °C, (B) 700 °C and (C) 800 °C.

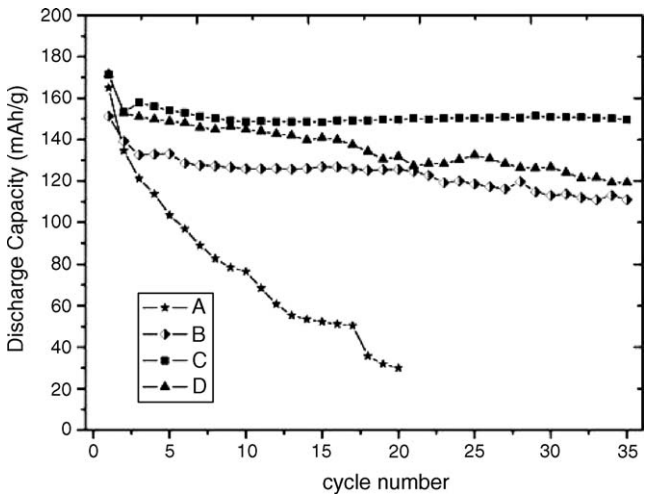

Fig. 8. Cycling performance of $Li_4Ti_5O_{12}$ prepared at 800 °C for different time with $R = 1.0$: (A) 12 h, (B) 16 h, (C) 20 h and (D) 24 h.

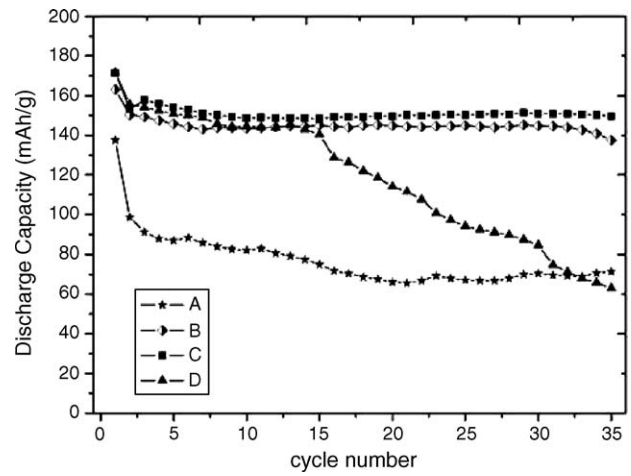

Fig. 9. Cycling performance of $Li_4Ti_5O_{12}$ synthesized at 800 °C for 20 h with different oxalic acid to titanium ratios R: (A) 0. 5, (B) 0.75, (C) 1.0 and (D) 1.5.

the lower crystallinity of the $Li_4Ti_5O_{12}$ and a large amount of anatase TiO_2 existing in the lower temperature powders. As the calcinations temperature was increased to 700 °C [Fig. 7(B)], there was an observed increase in the capacity. The initial discharge capacity increased to 171 mAh g^{-1}. The improved electrochemical characteristics of the material calcined 700 °C consistent with the XRD results, which show improved structural characteristics and there was only a little amount of TiO_2 in the final powder. But the cyclability of the material was poor. After 5 cycles, the discharge capacity was 158 mAh g^{-1}, and then the capacity decreased rapidly to 58 mAh g^{-1} after 20 cycles. The compound calcined at 800 °C [Fig. 7(C)] showed further increases in capacity and cyclability with a first discharge capacity of 171 mAh g^{-1} and a 35th cycle discharge capacity of 150 mAh g^{-1}. Improvement in the electrochemical properties for the 800 °C powder was mainly attributable to the complete crystallinity and without any miscellaneous phase in the final powders.

Fig. 8 shows the cycling behavior of the compounds calcined at 800 °C for different time with $R = 1.0$. As can be seen in Fig. 8, for the compound calcined at 800 °C for 12 h [Fig. 8(A)], the discharge capacity was 165 mAh g^{-1} in the first cycle and 30 mAh g^{-1} after 20 cycles. The reason may be there is anatase TiO_2 miscellaneous phase in the product. As calcination time was increased to 16 h [Fig. 8(B)], there was a corresponding increase in the discharge capacity and also the cyclability of the material, as explained in the previous section. The sample delivered a discharge capacity of 152 mAh g^{-1} in the first cycle and 123 mAh g^{-1} after 20 cycles. When the precursor calcined at 800 °C for 20 h, the material delivered the highest capacity as mentioned in Fig. 7(C). Further increasing the calcination time led to a decrease in capacity with a first cycle discharge capacity of 171 mAh g^{-1} and a 35th cycle discharge capacity of 125 mAh g^{-1}.

The homogeneity and crystallinity lattice parameter of the powder increases with increasing temperature, and hence, the cyclability increases. The cyclability of the cathode is improved by increasing the calcination temperature. In addition, capacity can decrease on increasing the temperature too high because the average particle size of the powder should also increase with increasing temperature; this would also affect the cyclability. Hence, it can be concluded from the above results that the optimal calcination time and temperature for $Li_4Ti_5O_{12}$ were 20 h and 800 °C, respectively.

Fig. 9 shows the cycling behavior of $Li_4Ti_5O_{12}$ electrodes calcined at 800 °C for 20 h with different R-values. As shown in Fig. 9(A), in the case of the gel precursor with $R = 0.5$, the sample $Li_4Ti_5O_{12}$ delivered an initial discharge capacity of 138 mAh g^{-1} and a discharge capacity of 71 mAh g^{-1} after 35 cycles. When the oxalic acid to titanium ratio was increased from 0.5 to 0.75 [Fig. 9(B)], the $Li_4Ti_5O_{12}$ shows an initial discharge capacity and 35th discharge capacity of 163 mAh g^{-1} and 138 mAh g^{-1}, respectively. A further increase in R to 1.0 [Fig. 9(C)] caused the prepared electrode to having the largest initial discharge capacity 171 mAh g^{-1}, and the 35th discharge capacity 150 mAh g^{-1}. When the R-value increased to 1.5, the capacity and cyclability decreased. It was 170 mAh g^{-1} in the first cycle and 63 mAh g^{-1} in the 35 cycles.

According to the results obtained from the SEM, the sample synthesized at a oxalic acid to titanium ratio of 1.0 had the smallest particles, also had the best electrochemical properties with a relatively large first discharge capacity 171 mAh g^{-1}. It is well known that the particle size, shape and homogeneity of electrode materials have a definite effect on the electrochemical properties. Among them, particle size is the main factor. According to Singhal et al. [21], smaller particles have shorter diffusion distances for intercalated Li-ions, resulting in a higher charge rate for intercalated anodes. Julien et al. [22] reported that, the decrease in the particle size of $Li_{4/3}Ti_{5/3}O_4$ spinels is unequivocally correlated with kinetics of grain formation using the proposed HEBM synthesis, which favors the tendency of small grains. Since electrochemical lithium intercalation and de-intercalation are in general limited by the rate of diffusion. The aforementioned features are important since smaller grain size can favor the lithium-ion mobility in the particles by reducing the ion-diffusion pathway. So we can adjust the particle size of the

samples by using different ratio of oxalic acid to titanium, thus controlling the electrochemical properties of $Li_4Ti_5O_{12}$ materials. In our paper, the suitable ratio of oxalic acid to titanium was validated to be 1.0.

4. Conclusions

Sub-micron $Li_4Ti_5O_{12}$ powders with narrow size distribution and superior dispersion was successfully synthesized by a sol–gel method using oxalic acid as a chelating agent. The results indicated that the prepared Li–Ti–O powders had a uniform morphology with average particle size about 200 nm, which is smaller than those obtained by solid-state method. The calcinations temperature, calcinations time and the content of oxalic acid have great effect on the electrochemical properly of the prepared spinel $Li_4Ti_5O_{12}$. In our study, the sample synthesized at 800 °C for 20 h with oxalic acid to titanium molar ratio $R = 1.0$ yielded the best capacity of 171 and 150 mAh g^{-1} for the first cycle and the 35th cycle, respectively at a current density of 0.5 mA cm^{-1} over a potential range between 1.0 and 2.5 V (versus Li). The $Li_4Ti_5O_{12}$ material prepared by oxalic acid-assisted solution method has excellent reliability and cyclability.

References

[1] T. Ohzuku, A. Ueda, N. Yamamoto, J. Electrochem. Soc. 142 (1995) 1431–1435.
[2] A.N. Jansen, A.J. Kahaian, K.D. Kepler, P.A. Nelson, K. Amine, D.W. Dees, D.R. Vissers, M.M. Thackeray, J. Power Sources 81–82 (1999) 902–905.
[3] G.X. Wang, D.H. Bradhurst, S.X. Dou, H.K. Liu, J. Power Sources (83) (1999) 156–161.
[4] M. Masatoshi, U. Satoshi, Y. Eriko, K. Keiji, I. Shinji, J. Power Sources (101) (2001) 53–59.
[5] K. Kanamura, T. Umegaki, H. Naito, Z. Takehara, T. Yao, J. Appl. Electrochem. 31 (2001) 73–78.
[6] D. Peramunage, K.M. Abraham, J. Electrochem. Soc. 145 (1998) 2615–2621.
[7] T. Brousse, P. Fragnaud, R. Marchand, D.M. Schleich, O. Bohnke, K. West, J. Power Sources 68 (1997) 412–415.
[8] K. Zaghib, M. Armand, M. Gauthier, J. Elecrochem. Soc. 9 (1998) 3135–3140.
[9] P.P. Prosini, R. Mancini, L. Petrucci, Solid State Ion. 144 (2001) 185–192.
[10] A. Du Pasquier, I. Plitz, S. Menocal, G. Amatucci, J. Power Sources 115 (2003) 171–178.
[11] A. Du Pasquier, A. Laforgue, P. Simon, J. Power Sources 125 (2004) 95–102.
[12] A. Du Pasquier, I. Plitz, J. Gural, S. Menocal, G. Amatucci, J. Power Sources 113 (2003) 62–71.
[13] S. Bach, J.P. Pereira-Ramos, N. Baffier, J. Power Sources 81–82 (1999) 273–276.
[14] C.M. Shen, X.G. Zhang, Y.K. Zhou, H.L. Li, Mater. Chem. Phys. 78 (2002) 437–441.
[15] Y.H. Rho, K. Kanamura, M. Fujisaki, J. Hamagami, S. Suda, T. Umegaki, Solid State Ion. 151 (2002) 151–157.
[16] Y.J. Hao, Q.Y. Lai, Z.H. Xu, X.Q. Liu, X.Y. Ji, Solid State Ion. 176 (2005) 1201–1206.
[17] A.J. Patil, M.H. Shinde, H.S. Potdar, Mater. Chem. Phys. 68 (2001) 7–16.
[18] R. Thirunakarana, K.T. Kimb, Y.M. Kangb, J.Y. Lee, Mater. Res. Bull. 40 (2005) 177–186.
[19] G. Ting-Kuo Fey, J.G. Chen, V. Subramanian, D.L. Huang, T. Akai, H. Masui, Mater. Chem. Phys. 79 (2003) 21–29.
[20] T.T. Fang, H.B. Lin, J.B. Hawang, J. Am. Ceram. Soc. 73 (1990) 3363.
[21] A. Singhal, G. Skandan, G. Amatucci, J. Power Sources 129 (2004) 38–44.
[22] C.M. Julien, M. Massot, K. Zaghib, J. Power Sources 136 (2004) 72–79.